

Annihilation of positronium atoms confined in mesoporous and macroporous SiO₂ filmsB. S. Cooper,¹ J.-P. Boilot,² C. Corbel,³ F. Guillemot,^{2,*} L. Gurung,¹ L. Liskay,³ and D. B. Cassidy¹¹*Department of Physics and Astronomy, University College London, Gower Street, London WC1E 6BT, United Kingdom*²*Groupe de Chimie du Solide, Laboratoire de Physique de la Matière Condensée, UMR CNRS 7643, Ecole Polytechnique, 91128 Palaiseau, France*³*DRF, IRFU and IRAMIS, CEA, University Paris-Saclay F-91191 Gif-sur-Yvette Cedex, France*

(Received 2 April 2018; revised manuscript received 2 May 2018; published 14 May 2018)

We report experiments in which positronium (Ps) atoms were created in thin, porous silica films containing isolated voids with diameters ranging from 5 to 75 nm. Ps lifetimes in the pore structures were measured directly via time-delayed laser excitation of $1^3S_1 \rightarrow 2^3P_J$ transitions. In a film containing 5-nm pores Ps was predominantly emitted into vacuum, with a small component of confined Ps with a lifetime of 75 ns also observed. In films with larger pores Ps atoms were not emitted into vacuum except from the film surface, and confined Ps lifetimes of ≈ 90 ns were measured with no dependence on the pore size. However, for such large pores, extended Tao-Eldrup (ETE)-type models predict Ps lifetimes close to the 142-ns vacuum value. Moreover, $1^3S_1 \rightarrow 2^3P_J$ excitation of Ps atoms inside the pores was found to result in annihilation and exhibited an extremely broad (≈ 10 THz) linewidth. We attribute these observations to a process in which nonthermal Ps atoms in the isolated voids become temporarily trapped in a series of surface states that dissociate following excitation. The occurrence of this mechanism is not necessarily apparent from ground-state Ps decay rates without some prior knowledge of the sample structure, and it precludes the application of ETE-type models as they do not take into account surface interactions other than pickoff annihilation.

DOI: [10.1103/PhysRevB.97.205302](https://doi.org/10.1103/PhysRevB.97.205302)**I. INTRODUCTION**

Highly porous materials such as silicate powders, ceramics, glasses, polymers, zeolites, metal organic frameworks, and aerogels [1,2] are used in many different ways, including low- k dielectrics for microelectronics [3], thermal insulators [4], catalysts [5], molecular sieves [6], drug delivery vehicles [7], gas storage cells for energy applications [8], and even superabsorbent powders for cleaning up oil spills [9].

The utility of porous materials often derives from their large specific surface areas, which in some cases can be as high as $1000 \text{ m}^2 \text{ g}^{-1}$. The development and synthesis of useful materials requires knowledge of their structure over a wide range of porosities, which are often characterized using gas absorption techniques [10–12]. Positronium (Ps) has also proved to be useful as a probe of porous materials [13].

Ps atoms confined in small volumes within insulating materials generally have decay rates that are related to the Ps-wall collision rate, which depends in part on the size and shape of the confining material. Remarkably, however, it has been found that the nature of the material does not have a significant effect on the pickoff decay rate [14], which means that generic models that focus on geometric properties can describe Ps decay rates in a wide range of materials. This type of model, known as the Tao-Eldrup (TE) model [15,16], has well-documented limitations [17–19] but, with various modifications, can successfully correlate Ps lifetimes directly

with free volumes [20–25]. This approach implicitly assumes that interactions with internal surfaces do not affect the Ps decay rate via mechanisms other than pickoff annihilation, e.g., via spin exchanging interactions with paramagnetic centers [26,27] or chemical quenching [28,29].

Here we report experiments in which Ps atoms were optically excited via the $1^3S_1 \rightarrow 2^3P_J$ transition while inside thin mesoporous and macroporous SiO₂ films [30]. We find that excitation of atoms immediately leads to annihilation and that the excitation line shapes are extremely broad (≈ 10 THz). In addition to this, the measured Ps lifetimes in the films are significantly shorter than predicted by extended TE (ETE) models [25] and, for pore sizes ≥ 32 nm, do not depend on the pore size. Our interpretation of these observations is that nonthermal Ps atoms in the isolated voids form a series of temporary surface states that control the Ps-surface scattering rate, lead to broadening of the excitation line shape, and facilitate the dissociation of Ps atoms excited to $n = 2$ levels.

II. EXPERIMENTAL METHODS**A. Ps production, excitation, and detection**

The experimental apparatus and techniques used in this work are explained in detail elsewhere [31]. Positrons obtained from the decay of a 1-GBq ²²Na source were moderated using neon [32] to generate a monoenergetic positron beam with approximately $5 \times 10^6 \text{ e}^+ \text{ s}^{-1}$. This beam was coupled to a two-stage [33] Surko-type positron trap [34] and a parabolic buncher [35] to produce pulses containing $\approx 10^5$ positrons with a spatial (temporal) width of 4 mm (3 ns) FWHM at a repetition rate of 1 Hz. The positron beam was guided to a target chamber

*Present address: Saint-Gobain Recherche, 39 quai Lucien Lefranc, 93303 Aubervilliers, France.

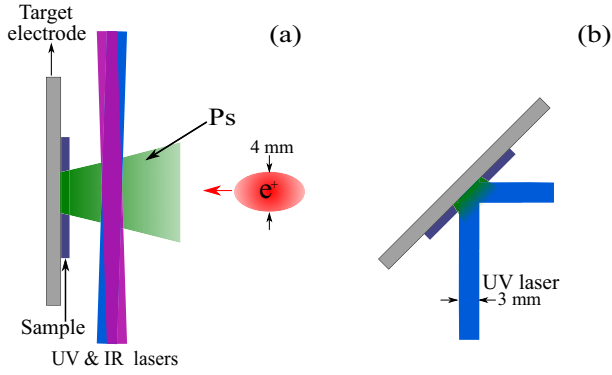


FIG. 1. Schematic of the target, positron, and laser beam orientations used for excitation of Ps atoms (a) in vacuum and (b) inside the silica film. In the case in (b) the laser covers the entire volume where Ps is produced in the target.

by an axial magnetic field of strength ≈ 80 G and could be implanted into various targets with energy E_B ranging from 0 to 5 keV, adjusted by biasing the target. The electric field in the Ps production region is also determined by the target bias. For all experiments reported here the silica films were at room temperature.

A pulsed ultraviolet (UV) Nd:YAG pumped dye laser (≈ 500 $\mu\text{J}/\text{pulse}$, $\Delta\nu = 85$ GHz, $\lambda = 243$ nm) was used to drive $1^3S_1 \rightarrow 2^3P_J$ transitions in Ps. The UV laser light was linearly polarized parallel to the beam axis. A second infrared (IR) dye laser (≈ 6 mJ/pulse, $\Delta\nu = 5$ GHz, $\lambda \approx 729$ nm) was used to photoionize 2^3P_J atoms. For the excitation and ionization of Ps in vacuum both the UV and IR laser beams were propagated parallel to the silica target surface, as shown in Fig. 1(a). To study confined Ps the sample was rotated by 45° relative to the beam axis, and the UV laser was directed into the target, as shown in Fig. 1(b). The IR laser was used in this configuration only to compare the UV annihilation signal with the photoionization signal.

The technique of single-shot positron annihilation lifetime spectroscopy (SSPALS) [36] was used to measure the production and excitation of Ps [31]. SSPALS relies on measuring annihilation radiation generated from a short pulse continuously, in effect developing a lifetime spectrum in “real time.” The resulting spectra are composed of an initial peak, caused by fast positron or singlet Ps annihilation (usually occurring on the timescale of the incident positron pulse), and a longer decay component due to the scintillator response, system noise, and, if present, Ps annihilation. The time resolution of this method is determined primarily by the properties of the scintillator used. In the present work we use both lead tungstate (PWO) [37] and lutetium yttrium oxyorthosilicate (LYSO) [38] scintillators attached to photomultiplier tubes to detect annihilation γ radiation. These scintillators have decay times of ≈ 12 and 40 ns, respectively, and are suitable for studies of Ps generated in mesoporous materials where Ps lifetimes may be comparable to the vacuum lifetime.

Figure 2 shows examples of SSPALS spectra obtained following positron implantation at 3 keV in an untreated Al target and in a mesoporous silica film (see Sec. II B). We expect that much more Ps will be produced by the silica film than the

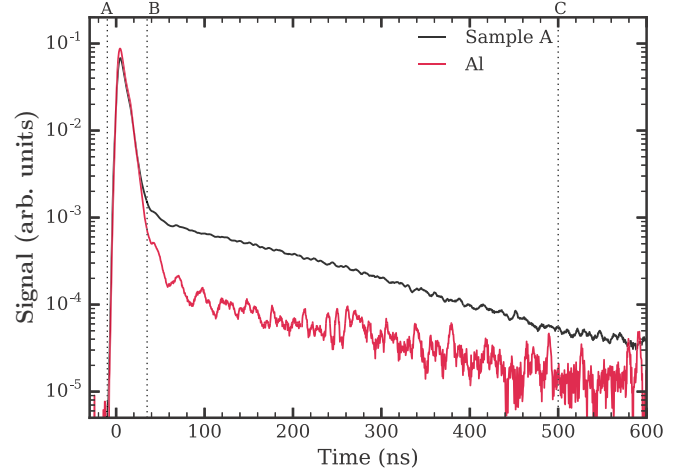


FIG. 2. Single-shot lifetime spectra measured with a 3 keV positron beam implanted into a porous silica film (sample A) and an untreated Al plate. The data were recorded using a PWO detector. The analysis time windows A, B, and C (-10 , 40, and 500 ns, respectively) are indicated by the dotted vertical lines. The Al spectrum is taken to be the instrument function used in the fitting procedure described in the text.

Al target, which is confirmed by the data, which clearly show increased annihilation radiation at later times in the silica case. We quantify the amount of long-lived Ps present using the parameter f_d [36], which is defined as

$$f_d = \int_B^C V(t) dt / \int_A^C V(t) dt, \quad (1)$$

where $V(t)$ is the detector output voltage and the time windows defined by A , B , and C will be chosen according to the detector being used and the process being studied [31]. Here we use $A = -10$, $B = 40$, and $C = 500$ ns for PWO and $A = -10$, $B = 120$, and $C = 700$ ns for LYSO [38]. For PWO time windows a rough approximation of the Ps fraction is $f_{Ps} \approx 2 \times (f_d - f_{bk})$, where f_{bk} refers to the background signal [39]. Since all scintillators have a finite (exponential) decay time, f_{bk} will not be zero, even if no Ps is formed. Often, one may ignore this background contribution, but in the present work the signal obtained from confined Ps is small, and so it has to be taken into account. We assume that a negligible amount of Ps will be generated on the Al surface for $E_B = 3$ keV, and the Al spectrum in Fig. 2 is taken to be the background signal, yielding $f_{bk} = 3.5 \pm 0.7\%$.

Laser-induced changes in lifetime spectra are quantified by the parameter S_γ , which is given by

$$S_\gamma = (f_{d(\text{off})} - f_{d(\text{on})}) / f_{d(\text{off})}, \quad (2)$$

where on and off refer to whether the UV laser is on or off resonance [31].

The measured SSPALS signal is the γ -ray flux convolved with the full response of the detection system; we refer to the latter as the instrument function (IF). For the present purposes we approximate the IF as an SSPALS spectrum obtained when no Ps is produced [40]. This will contain a component due to fast annihilation events and so is not the true IF, as this component will change when some of the positrons form Ps

atoms. However, by scaling the IF and convolving it with an exponential function one may fit SSPALS spectra that contain a Ps component and thus determine Ps lifetimes. This procedure, which we refer to as instrument function fitting (IFF), does not discriminate between Ps in vacuum or inside a porous network. We note that one can generate an analytical approximation [41] of the IF instead of relying on a measurement assumed to be free of significant Ps production. Fits performed using such a function were in agreement with our measurements, but with larger error bars due to the extra fitting parameters.

Ps lifetimes can also be measured using delayed laser excitation (DLE), in which case we use the notation τ_{DLE} . In this method photoexcitation of the $1^3S_1 \rightarrow 2^3P_J$ transition is followed by annihilation, resulting either from the sample properties (as in the present case, see Sec. III) or from photoionization using a second (IR) laser pulse [31]. The amount of excess annihilation radiation in the lifetime spectrum immediately after the laser has been fired depends on the number of Ps atoms remaining in the sample. Thus, lifetimes are obtained from the correlation between the areas of the excess annihilation peaks and the UV laser delay time.

B. Porous silica films

The experiments we describe here were conducted using four samples (henceforth labeled A–D) with different pore sizes and porosities, as listed in Table I.

All films were prepared by the sol-gel method [2] using tetraethylorthosilicate (TEOS) as a silica precursor and a sacrificial porogen. The sol was deposited by spin coating on a silicon single-crystal substrate, and the porogen was removed by heating the samples in air. The film preparation for sample A differs from that used for samples B, C, and D. The porosity of sample A was generated using micelles of nonionic Pluronic F-127 triblock copolymer as a surfactant [42]. Porous films of approximately $1 \mu\text{m}$ thickness were formed by removing the pore-generating agent by heating the samples to 450°C in air.

Samples B, C, and D were prepared using poly(methyl methacrylate) (PMMA) latex nanoparticles with diameters of 32, 51, and 75 nm as a sacrificial template [43]. The template was removed by heating to 450°C (sample B) and 600°C (samples C and D) in air. Positron measurements showed no difference between identically prepared films heated to 450°C and 600°C . Samples B, C, and D were approximately 300 nm thick. For each pore size the full width at half maximum of

TABLE I. Properties of the four samples used in the present work. The porosity P and mean pore diameter D were determined as explained in the text. Ps lifetimes obtained from both instrument function fitting (τ_{IFF}) and delayed laser excitation (τ_{DLE}) are shown. The value of f_d was measured using a PWO detector and a positron beam energy of 3 keV and includes background subtraction (see Sec. II A).

Sample	P (%)	D (nm)	τ_{IFF} (ns)	τ_{DLE} (ns)	f_d (%)
A	50	5	146 ± 3	75 ± 5	14.2
B	40	32	83 ± 5	91 ± 3	3.2
C	40	51	91 ± 6	89 ± 2	1.6
D	40	75	84 ± 6	89 ± 2	1.8

the size distribution of the latex nanoparticles was measured [43,44] using dynamic light scattering and was found to be less than 10 nm. The pore size distributions in the films were experimentally determined via spectroscopic ellipsometry and were found to be indistinguishable from the size distribution of the latex nanoparticles. After removal of the porogen the films are known to shrink slightly, and the shape of the pores becomes partially flattened, although the present experiment would not be sensitive to such changes. The pore size and porosity of all samples as determined from spectroscopic ellipsometry are listed in Table I.

Films prepared under the same conditions as those used in this work were studied by Guillemot and coworkers [43]. A disordered pore distribution was observed via scanning electron microscopy imaging, and Fourier transform infrared spectroscopy showed that curing the films at increasing temperatures up to 450°C results in a progressive decrease of the intensity for the silanol Si-OH stretching band (950 cm^{-1}) and for the hydroxyl stretching band (3000 cm^{-1}). The fact that some fraction of silanol groups remains after heating at 450°C suggests that a few percent of microporosity subsists in the silica walls in the PMMA-templated films [43]. Positron-based characterization of these films was also performed [45], in which the samples were heated to 450°C with a $10^\circ\text{C}/\text{min}$ heating rate a few minutes before installation into a UHV system. Earlier studies on mesoporous films have shown that reheating porous silica films improves the reproducibility of positron measurements, probably due to the removal of water that penetrates into the pore matrix during aging in ambient atmosphere. In the present work the samples were *not* reheated prior to insertion in the vacuum system. Moreover, they had been stored for several years in atmosphere before being used.

III. RESULTS AND DISCUSSION

Energetic positrons implanted into insulating materials can form Ps atoms via several different mechanisms [46], either in the bulk material or following positron diffusion to a surface [47–49]. In porous materials it is possible for Ps atoms in internal open volumes to escape into vacuum or become localized, depending on the pore geometry and interconnectivity [50]. Ps emission into vacuum is more likely to occur from materials with high porosity and small pores [45], and films similar to sample A are often used as Ps sources [51].

Figure 3 shows line shapes of $1^3S_1 \rightarrow 2^3P_J$ transitions of Ps driven in vacuum [see Fig. 1(a)] for different positron implantation energies and silica targets. The data presented in Fig. 3(a) were recorded using sample A and show Doppler profiles consistent with those previously obtained from similar films [52]. Small-pore films typically exhibit collisional cooling as the positron beam implantation energy is increased, which in this case is indicated by a small narrowing of the line shape.

The data shown in Fig. 3(b) were recorded using sample B. In this case the signal rapidly drops off as the positron beam energy is increased, indicating a reduction in the number of Ps atoms emitted into vacuum. The signal obtained for a positron beam energy of 0.2 keV is attributed to Ps emitted directly from the silica surface. In this case there is no Ps cooling, as evidenced by the much broader Doppler profile.

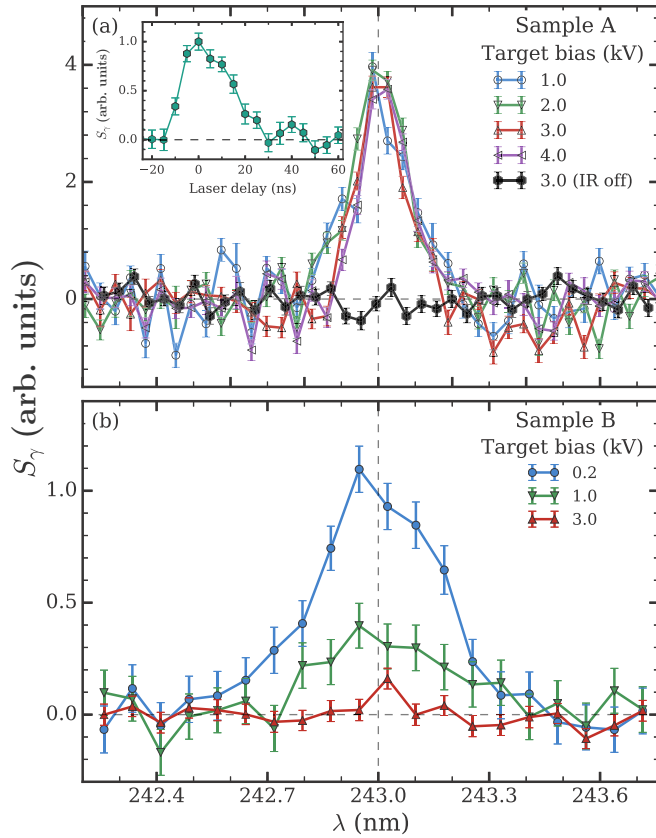


FIG. 3. The $1^3S_1 \rightarrow 2^3P_J$ transitions driven in Ps atoms in vacuum for different positron beam energies and using (a) sample A and (b) sample B. A second (IR) laser tuned to 729 nm was used to photoionize excited states, except where indicated. The inset in (a) shows a scan of the time delay between the positron pulse and lasers on resonance. The line shapes were recorded using a LYSO detector, and the delay scan was recorded using a PWO detector.

It should be remembered that, by its definition, S_γ is a measure of the fraction of Ps atoms present that are excited by the applied laser light, and therefore, it is not directly sensitive to the absolute number of Ps atoms produced by the positron pulse. However, if Ps atoms are generated that are not excited by the laser, then S_γ will decrease accordingly. Thus, the data shown in Fig. 3 can be interpreted in the following way: the nearly constant value of S_γ in Fig. 3(a) means that the fraction of Ps produced that is emitted into vacuum has almost no dependence on the beam energy, whereas the drop in S_γ for increasing beam energy seen in Fig. 3(b) means that a lower fraction of the produced atoms interact with the laser light. This can be explained if long-lived Ps atoms are created but are not emitted into vacuum or if they are emitted with very high speeds. In general the energy of Ps atoms emitted from silica films will *decrease* as E_B is increased, indicating that confined Ps is produced. Very similar data were obtained using samples C and D, and these observations are consistent with measurements [45] showing that Ps emission via the pore network in similar films becomes much more efficient above a porosity threshold of approximately 60%.

Figure 4(a) shows a lifetime spectrum measured for positrons implanted into sample A at an energy of 3 keV. IFF

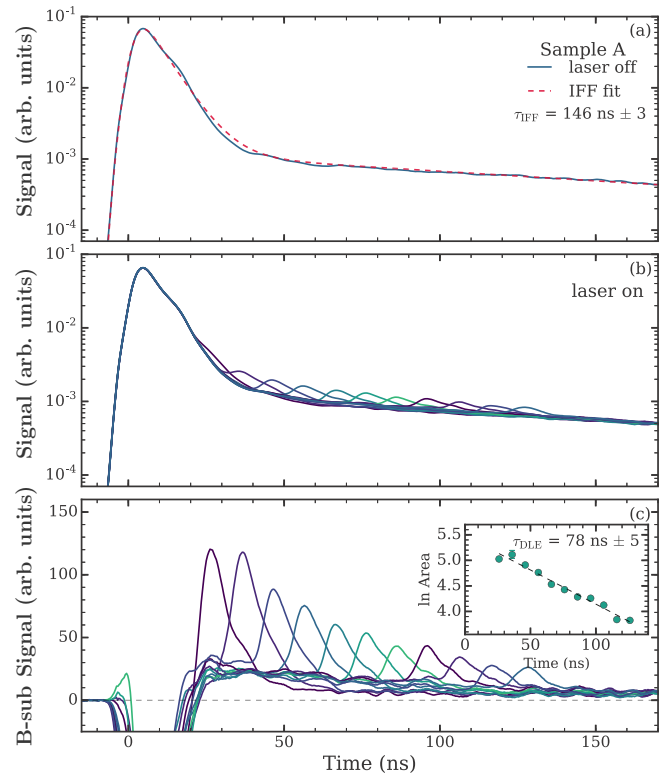


FIG. 4. (a) Single-shot lifetime spectra (solid line) recorded using sample A (see Table I) and the fit (red dashed line) used to determine τ_{IFF} . (b) Lifetime spectra in which the UV laser is fired at different delays from 30 to 130 ns in 10-ns intervals as described in the text, and (c) difference signal between lifetime spectra with and without laser irradiation plotted on a linear scale. The inset in (c) shows the integrated areas of the laser-induced peaks and the fit (straight dashed line) used to determine τ_{DLE} . These data were recorded using a PWO detector.

using these data yields $\tau_{\text{IFF}} = 146 \pm 3$ ns, i.e., the Ps vacuum lifetime. This is consistent with the observation that most Ps produced in this sample is emitted into vacuum [see Fig. 3(a)]. Figure 5 shows IFF data for spectra generated using samples B, C, and D, yielding lifetimes of 83 ± 5 , 91 ± 6 , and 84 ± 6 ns, respectively.

DLE data for sample A are shown in Fig. 4(b), using the sample orientation shown in Fig. 1(b) (i.e., Ps excitation inside the sample). The laser-induced peaks in the lifetime spectra ranging from 30 to 130 ns in 10-ns intervals are clearly visible. The same data are shown in Fig. 4(c) with the background (no laser) spectrum subtracted. The background-subtracted areas of the laser-induced excess γ radiation peaks are approximately proportional to the number of Ps atoms present. Thus, fitting an exponential function to these data, as shown in the inset in Fig. 4(c), yields a lifetime (in this case $\tau_{\text{DLE}} = 75 \pm 5$ ns). Figure 6 shows background-subtracted DLE data obtained in the same way for samples B, C, and D, yielding lifetimes of 91 ± 3 , 89 ± 2 , and 89 ± 2 ns, respectively.

We note that similarly produced [42] silica films were previously studied using Ps reemission and lifetime spectroscopy [53]. In that work the lifetime of Ps inside the pores of a mesoporous film nominally identical to sample A was found

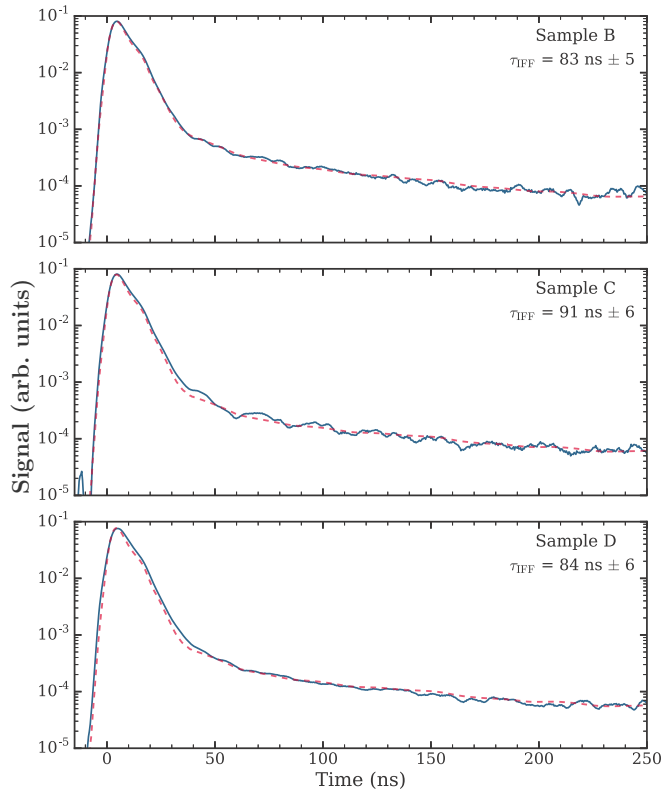


FIG. 5. Lifetime spectra (solid lines) and IFF (dashed lines) for samples B (32 nm), C (51 nm), and D (75 nm). The τ_{IFF} values obtained from the fits are shown in the legends. These data were recorded using a PWO detector.

to be 74 ± 1 ns. The good agreement between the current and previous measurements shows that the sample properties are resilient to long-term storage in atmosphere, even without heating immediately before use.

A key feature of the DLE method employed in this work is that it is sensitive *only* to Ps inside the porous material. The reason for this is that Ps excited via $1^3S_1 \rightarrow 2^3P_J$ transitions in vacuum will generally decay back to the 1^3S_1 ground state, resulting in a negligible change in the total decay rate. Because of Zeeman and Stark mixing it is possible for atoms excited in this way to decay to the short-lived 1^1S_0 singlet ground state [54], which would provide an annihilation signal [55]. However, the electric fields and laser light polarization used in this work were such that this effect was negligible [56]. This is confirmed by the “IR off” curve in Fig. 3(a), where no signal was observed when Ps was excited in vacuum if the IR photoionization laser was not used.

Conversely, Ps excited inside the sample was found to annihilate without the presence of an additional laser, giving rise to laser-induced excess annihilation peaks in the lifetime spectra [see Figs. 4(c) and 6]. The shape of these peaks is not presently understood, and in particular it is not known why the sample C curves are different from the others. It is possible that dissociated positrons undergo complicated surface interactions before annihilation and that the peak shapes contain information about this process, but more studies are required to understand the observed line shapes.

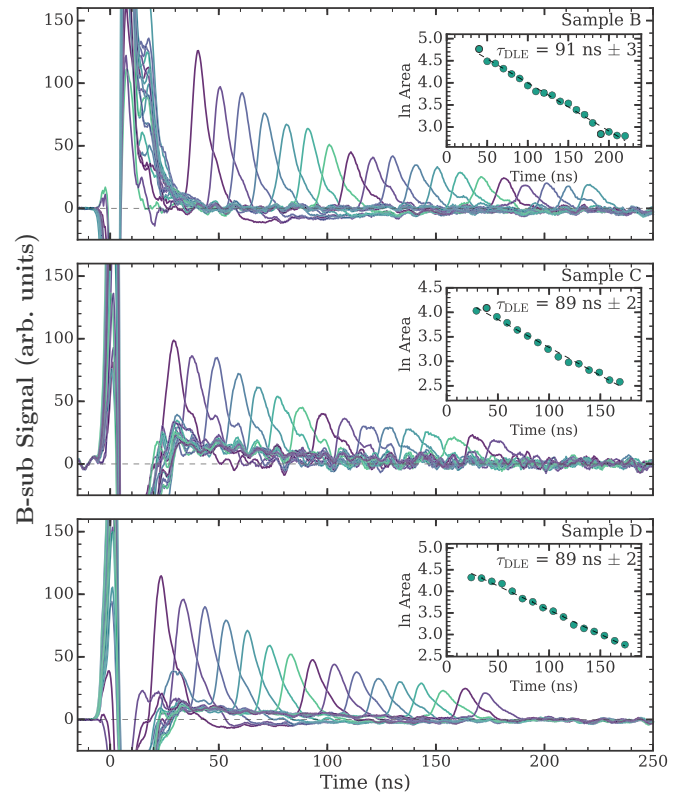


FIG. 6. Background-subtracted laser-induced peaks for samples B (32 nm), C (51 nm), and D (75 nm) as indicated. The insets show the integrated areas of the laser-induced peaks and the fits (dashed lines) used to determine the Ps lifetimes τ_{DLE} given in Table I. These data were recorded using a PWO detector.

As is evident from Fig. 4, the DLE signal obtained with sample A persists for up to 130 ns after the positron implantation. However, the efficient vacuum emission observed from the same sample suggests that Ps is emitted on a timescale much shorter than the Ps lifetime. Measurements of the Ps emission time profile are shown in the inset of Fig. 3(a) and show that Ps can be detected in vacuum over a time span of ≈ 40 ns. This is consistent with the Ps flight time through the laser and is much shorter than the range over which DLE signals are observed. The emission time from similar samples has been measured directly in time-of-flight experiments [57] and was found to be on the order of 10 ns. Thus, these data show that the DLE signal is primarily due to Ps that is permanently confined in the sample, implying that this sample has both open and closed pore networks. A comparison of the DLE signals observed for sample A (Fig. 4) and for the large-pore samples (Fig. 6) indicates that the confined Ps fraction in all cases is of the same magnitude; that is, on the order of a few percent of implanted positrons form confined Ps.

The $1^3S_1 \rightarrow 2^3P_J$ excitation line shapes observed for confined Ps in all four samples are extremely broad. An example of this, measured using sample B, is shown in Fig. 7. These data show $1^3S_1 \rightarrow 2^3P_J$ line shapes recorded with Ps excited in vacuum [see Fig. 1(a)], and with Ps atoms confined in the sample [see Fig. 1(b)]. Although very broad and not very reproducible in terms of the shape, the line shapes measured for confined Ps are, nevertheless, resonant at

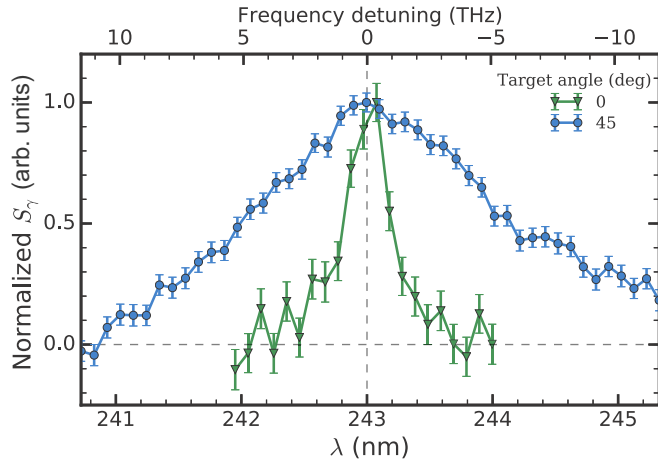


FIG. 7. Normalized $1^3S_1 \rightarrow 2^3P_J$ line shapes measured using sample B for Ps in vacuum (target angle of 0°) and for Ps confined in isolated pores (target angle of 45°). These data were recorded using a LYSO detector.

≈ 243 nm. This proves that the annihilation mechanism is not caused by nonresonant laser-induced processes that can quench ground-state atoms, such as the production of paramagnetic centers [26,58,59].

The vacuum Ps data in Fig. 7 were recorded with a positron beam energy of 0.5 keV. This produces Ps directly from the SiO_2 surface that is emitted with no significant collisional cooling and has an energy on the order of a few eV [60]. The vacuum line shape is therefore maximally broad with respect to Doppler effects, and the extreme broadening of the transitions observed for confined Ps must be caused by some other mechanism.

In Fig. 8 we compare the IFF and DLE lifetime measurements reported in Table I with the ETE prediction as given by Wada and Hyodo [25] (which are essentially indistinguishable from the models of Gidley and coworkers [22] and others [23]). This curve describes thermalized Ps at 300 K and can therefore

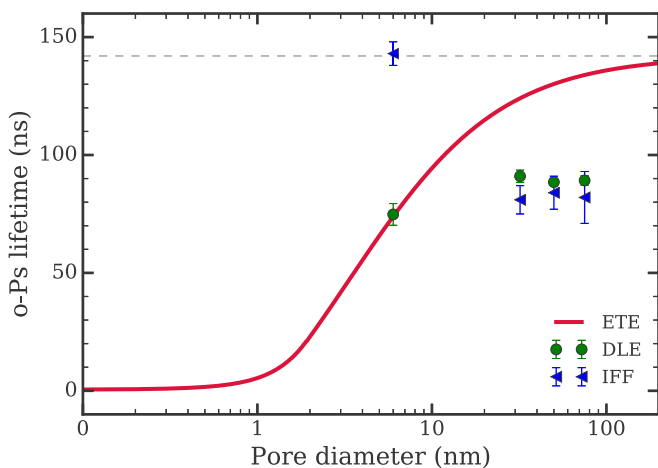


FIG. 8. Ps lifetimes in all samples as derived from DLE (circles) and IFF (triangles). Also shown is the ETE model prediction derived using the approximation of Wada and Hyodo [25]. The dashed horizontal line indicates the Ps vacuum lifetime.

give only an approximate prediction for our data; in sample A, Ps will thermalize in less than 10 ns, whereas in the other samples thermalization will take much longer (50–100 ns) [61]. Hotter Ps will exhibit a shorter lifetime [22], but this effect is much smaller in the “classical” regime of large pores. For nonthermal Ps we would expect ETE predictions somewhat lower than shown in Fig. 8, with lifetimes in larger-pore samples reduced to (at most) 100 ns. The lifetimes would still depend on the pore size.

It is evident from Fig. 8 that the IFF and DLE methods give consistent results for the large-pore samples (B–D) but that there is a large disagreement for the small-pore sample (A). This occurs because the IFF method is sensitive to all Ps decays and thus detects both confined and vacuum Ps, while DLE detects only confined Ps. In the large-pore measurements there is only confined Ps, and thus, the two methods agree. Most of the Ps atoms created in sample A are emitted into vacuum; IFF is dominated by this signal and therefore gives a value close to the vacuum lifetime.

There are several aspects of our measurements that are presently not explained. These are the nature of the quenching/dissociation mechanism that causes annihilation upon excitation and the extreme broadening of the transition linewidth, the lifetime disagreement with ETE predictions, and the fact that the observed ≈ 90 ns lifetimes in the larger-pore samples do not depend on the pore sizes. Nevertheless, some of the properties of the underlying physical mechanism(s) can be deduced from our measurements:

(1) An almost identical DLE signal from confined Ps is generated if an IR laser is used along with the UV light to photoionize excited states; the observed signal does not increase significantly when both lasers are used, indicating that the quenching process is roughly as efficient as photoionization. The IR radiation fluence used was sufficient to approach saturation of the ionization process [56], and we therefore conclude that most confined atoms that are excited do subsequently annihilate.

(2) Ps atoms that are not confined have been probed inside porous silica films similar to sample A in previous experiments [62]. In this work excited atoms did not annihilate unless an ionization laser was used, and line broadening was not observed. Conversely, in all present cases involving permanently confined Ps, we do observe these effects. This implies that the quenching mechanism is connected to the isolated pore structures, either due to the presence of contaminants or via a physical mechanism that occurs exclusively therein.

(3) Since excitation of 2^3P_J levels will not ordinarily result in an increased annihilation rate [56], the extreme width of the observed $1^3S_1 \rightarrow 2^3P_J$ line shapes coupled with the fact that excitation leads directly to annihilation indicates that the Ps is strongly interacting with a surface during the excitation. The existence of the annihilation signal indicates that excited surface states are able to dissociate or engage in some other decay process.

(4) The observed Ps lifetimes in samples B, C, and D are all shorter than ETE predictions [25] and are all essentially the same (≈ 90 ns), with no dependence on the pore size. This implies that the quenching mechanism is not mediated by direct surface interactions at a rate determined by the Ps-surface scattering. Instead, this observation suggests that Ps exists in

surface states that give rise to similar Ps-surface interaction rates, regardless of the pore size.

The seemingly conflicting observations of extreme line broadening (suggesting a strong Ps-surface interaction) and relatively long lifetimes (indicating a weak Ps-surface interaction) can be reconciled if Ps atoms become captured in surface states but are continuously trapped and detrapped during the thermalization process. This can occur only in a confining geometry where multiple interactions with surfaces are inevitable. Presently, we can only speculate as to the Ps-surface attachment mechanism, but the resonant attachment of positrons to molecules is a well-known phenomenon [63], and weak Ps-atom binding is expected to be a common phenomenon [64–66].

Temporary Ps attachment can result in a surface scattering rate that does not depend strongly on the pore size but instead is determined primarily by the trapping and detrapping rates. Then, for similar surface conditions, similar Ps lifetimes will be observed, even for very different pore sizes. However, in sample A the observed ≈ 75 -ns lifetime is shorter than is observed for the other cases, which does not agree with this hypothesis. This may be explained by the fact that in sample A the Ps de Broglie wavelength is much closer to the pore size than it is in the other samples [52,67], which can modify the surface interaction rate and reduce the lifetime to the ETE prediction.

The measured $1^3S_1 \rightarrow 2^3P_J$ linewidth will be affected by temporary surface interactions if the excitation Rabi frequency is comparable to or less than the average scattering rate; the applied laser fluences result in Rabi frequencies on the order of a few gigahertz [57]. The surface residence time for a mechanism of this type must be short (subnanosecond) to account for the observed lifetimes but will still have a large effect on the effective scattering rate, which would be much faster than the Rabi frequency for realistic experimental parameters.

The precise nature of the broadening mechanism remains unclear, but it has some characteristics consistent with chemical quenching [68]. In this process Ps is thought to form a chemical bond with a molecule, leading to an increased annihilation rate. Chemical quenching of Ps has been observed for Ps interacting with NO_2 molecules adsorbed on the internal surfaces of silica aerogel and was found to have a cross section several orders of magnitude larger than that of spin conversion [69]. As pointed out by Hyodo and coworkers [27], it has not been demonstrated that a stable compound is formed in this process (which they refer to as attachment quenching), and they suggest that it is more likely that the Ps forms a resonance state with the molecule. If attached Ps atoms are

excited, they may no longer exist in a bound state, leading to dissociation as we have observed. This is consistent with the fact that chemical quenching is characterized by an increase in the (ground-state) Ps momentum, as observed via the angular correlation of annihilation radiation [69].

Additional work is required to fully describe the physical mechanisms underlying the surface interaction and quenching processes. To study these effects further it would be beneficial to perform systematic measurements in a series of well-characterized samples. Experiments performed at different temperatures can confirm whether or not the observed effects are mediated by nonthermal Ps, and films made from materials other than silica [70] are likely to exhibit different surface attachment properties and will contain different contaminants. It may also be instructive to perform laser excitation measurements of Ps in surface states on single-crystal quartz samples [71,72]. Ps thermalization rates must be strongly affected by a surface trapping-detrapping mechanism, and it is therefore of interest to directly measure this for confined Ps using various energy-time selection methods [61,73–76].

IV. CONCLUSIONS

The experiments we have described here reveal the existence of decay pathways that may affect the applicability of ETE-type models used in positron-based characterization methods [13]. Some of the effects of surface chemistry and morphology on ground-state Ps atoms have been previously characterized [77–80], but the excited-state effects we observed are unique. Without prior knowledge of the pore structure it may not be apparent from the Ps decay rates that these processes are occurring. In the present case the pore sizes were known well enough that the almost constant lifetimes were obviously anomalous, and laser excitation has revealed unexplained broadening and annihilation. If they are common in isolated void networks, the observed effects have implications for proposed schemes to perform laser cooling on confined Ps atoms [81] or to produce Bose-Einstein condensed Ps in isolated cavities [82].

ACKNOWLEDGMENTS

We gratefully acknowledge A. M. Alonso and A. Deller for work related to earlier aspects of the experiment and G. Gribakin and S. D. Hogan for helpful discussions. This work was funded in part by the EPSRC (Grant No. EP/R006474/1).

[1] D. W. Bruce, D. O'Hare, and R. I. Walton, *Porous Materials*, Inorganic Materials Series (Wiley, Hoboken, NJ, 2011).
 [2] C. J. Brinker and G. W. Scherer, *Sol-Gel Science: The Physics and Chemistry of Sol-Gel Processing* (Elsevier, San Diego, 2013).
 [3] M. P. Petkov, M. H. Weber, K. G. Lynn, and K. P. Rodbell, Probing capped and uncapped mesoporous low-dielectric constant films using positron annihilation lifetime spectroscopy, *Appl. Phys. Lett.* **77**, 2470 (2000).

[4] J.-J. Zhao, Y.-Y. Duan, X.-D. Wang, and B.-X. Wang, Experimental and analytical analyses of the thermal conductivities and high-temperature characteristics of silica aerogels based on microstructures, *J. Phys. D* **46**, 015304 (2013).
 [5] X. S. Zhao, X. Y. Bao, W. Guo, and F. Y. Lee, Immobilizing catalysts on porous materials, *Mater. Today* **9**, 32 (2006).
 [6] C. T. Kresge, M. E. Leonowicz, W. J. Roth, J. C. Vartuli, and J. S. Beck, Ordered mesoporous molecular sieves synthesized

- by a liquid-crystal template mechanism, *Nature (London)* **359**, 710 (1992).
- [7] E. J. Anglin, L. Cheng, W. R. Freeman, and M. J. Sailor, Porous silicon in drug delivery devices and materials, *Adv. Drug Delivery Rev.* **60**, 1266 (2008).
- [8] D. N. Dybtsev, H. Chun, S. H. Yoon, D. Kim, and K. Kim, Microporous manganese formate: A simple metal organic porous material with high framework stability and highly selective gas sorption properties, *J. Am. Chem. Soc.* **126**, 32 (2004).
- [9] M. O. Adebajo, R. L. Frost, J. T. Klopogge, O. Carmody, and S. Kokot, Porous materials for oil spill cleanup: A review of synthesis and absorbing properties, *J. Porous Mater.* **10**, 159 (2003).
- [10] S. Brunauer, P. H. Emmett, and E. Teller, Adsorption of gases in multimolecular layers, *J. Am. Chem. Soc.* **60**, 309 (1938).
- [11] E. P. Barrett, L. G. Joyner, and P. P. Halenda, The determination of pore volume and area distributions in porous substances. I. Computations from nitrogen isotherms, *J. Am. Chem. Soc.* **73**, 373 (1951).
- [12] W. C. Conner, J. F. Cevallos-Candau, E. L. Weist, J. Pajares, S. Mendioroz, and A. Cortes, Characterization of pore structure: Porosimetry and sorption, *Langmuir* **2**, 151 (1986).
- [13] D. W. Gidley, H. G. Peng, and R. S. Vallery, Positron annihilation as a method to characterize porous materials, *Annu. Rev. Mater. Res.* **36**, 49 (2006).
- [14] K. Wada, F. Saito, N. Shinohara, and T. Hyodo, Pick-off quenching probability of ortho-positronium per collision with atoms and molecules, *Eur. Phys. J. D* **66**, 108 (2012).
- [15] S. J. Tao, The formation of positronium in molecular substances, *Appl. Phys.* **10**, 67 (1976).
- [16] M. Eldrup, D. Lightbody, and J. N. Sherwood, The temperature dependence of positron lifetimes in solid pivalic acid, *Chem. Phys.* **63**, 51 (1981).
- [17] Z. Yu, J. D. McGervey, A. M. Jamieson, and R. Simha, Can positron annihilation lifetime spectroscopy measure the free-volume hole size distribution in amorphous polymers? *Macromolecules* **28**, 6268 (1995).
- [18] Y. C. Jean, Comments on the paper can positron annihilation lifetime spectroscopy measure the free-volume hole size distribution in amorphous polymers? *Macromolecules* **29**, 5756 (1996).
- [19] R. Zaleski, Ortho-positronium localization in pores of vycor glass at low temperature, *J. Phys. Conf. Ser.* **443**, 012062 (2013).
- [20] H. Nakanishi and Y. Ujihira, Application of positron annihilation to the characterization of zeolites, *J. Phys. Chem.* **86**, 4446 (1982).
- [21] T. Goworek, K. Ciesielski, B. Jasiaska, and J. Wawryszczuk, Positronium states in the pores of silica gel, *Chem. Phys.* **230**, 305 (1998).
- [22] D. W. Gidley, W. E. Frieze, T. L. Dull, A. F. Yee, E. T. Ryan, and H.-M. Ho, Positronium annihilation in mesoporous thin films, *Phys. Rev. B* **60**, R5157 (1999).
- [23] K. Ito, H. Nakanishi, and Y. Ujihira, Extension of the equation for the annihilation lifetime of ortho-positronium at a cavity larger than 1 nm in radius, *J. Phys. Chem. B* **103**, 4555 (1999).
- [24] Y. C. Jean, J. D. V. Horn, W.-S. Hung, and K.-R. Lee, Perspective of positron annihilation spectroscopy in polymers, *Macromolecules* **46**, 7133 (2013).
- [25] K. Wada and T. Hyodo, A simple shape-free model for pore-size estimation with positron annihilation lifetime spectroscopy, *J. Phys. Conf. Ser.* **443**, 012003 (2013).
- [26] D. B. Cassidy, K. T. Yokoyama, S. H. M. Deng, D. L. Griscom, H. Miyadera, H. W. K. Tom, C. M. Varma, and A. P. Mills, Jr., Positronium as a probe of transient paramagnetic centers in α -SiO₂, *Phys. Rev. B* **75**, 085415 (2007).
- [27] T. Hyodo, T. Nakayama, H. Saito, F. Saito, and K. Wada, The quenching of ortho-positronium, *Phys. Status Solidi C* **6**, 2497 (2009).
- [28] S. Y. Chuang and S. J. Tao, Study of inhibition and quenching of positronium by iodine and CCl₄, *J. Chem. Phys.* **52**, 749 (1970).
- [29] C. Li, H. J. Zhang, and Z. Q. Chen, Chemical quenching of positronium in Fe₂O₃/Al₂O₃ catalysts, *Appl. Surf. Sci.* **256**, 6801 (2010).
- [30] Note that we adhere to the International Union of Pure and Applied Chemistry convention regarding porous materials, which defines microporous, mesoporous, and macroporous materials as those containing pores with diameters of less than 2 nm, between 2 and 50 nm, and greater than 50 nm, respectively.
- [31] B. S. Cooper, A. M. Alonso, A. Deller, T. E. Wall, and D. B. Cassidy, A trap-based pulsed positron beam optimised for positronium laser spectroscopy, *Rev. Sci. Instrum.* **86**, 103101 (2015).
- [32] A. P. Mills, Jr. and E. M. Gullikson, Solid neon moderator for producing slow positrons, *Appl. Phys. Lett.* **49**, 1121 (1986).
- [33] R. G. Greaves and J. Moxom, Design and performance of a trap based positron beam source, in *Non-Neutral Plasma Physics V: Workshop on Non-Neutral Plasmas*, AIP Conf. Proc. No. 692 (AIP, New York, 2003), p. 140.
- [34] J. R. Danielson, D. H. E. Dubin, R. G. Greaves, and C. M. Surko, Plasma and trap-based techniques for science with positrons, *Rev. Mod. Phys.* **87**, 247 (2015).
- [35] A. P. Mills, Jr., Time bunching of slow positrons for annihilation lifetime and pulsed laser photon absorption experiments, *Appl. Phys.* **22**, 273 (1980).
- [36] D. B. Cassidy, S. H. M. Deng, H. K. M. Tanaka, and A. P. Mills, Jr., Single shot positron annihilation lifetime spectroscopy, *Appl. Phys. Lett.* **88**, 194105 (2006).
- [37] D. B. Cassidy and A. P. Mills, Jr., A fast detector for single-shot positron annihilation lifetime spectroscopy, *Nucl. Instrum. Methods Phys. Res., Sect. A* **580**, 1338 (2007).
- [38] A. M. Alonso, B. S. Cooper, A. Deller, and D. B. Cassidy, Single-shot positron annihilation lifetime spectroscopy with LYSO scintillators, *Nucl. Instrum. Methods Phys. Res., Sect. A* **828**, 163 (2016).
- [39] D. B. Cassidy, T. H. Hisakado, H. W. K. Tom, and A. P. Mills, Jr., Positronium formation via excitonlike states on Si and Ge surfaces, *Phys. Rev. B* **84**, 195312 (2011).
- [40] D. B. Cassidy, S. H. M. Deng, R. G. Greaves, T. Maruo, N. Nishiyama, J. B. Snyder, H. K. M. Tanaka, and A. P. Mills, Jr., Experiments with a High-Density Positronium Gas, *Phys. Rev. Lett.* **95**, 195006 (2005).
- [41] C. J. Baker, D. Edwards, C. A. Isaac, H. H. Telle, D. P. van der Werf, and M. Charlton, Excitation of positronium: From the ground state to Rydberg levels, *J. Phys. B* **51**, 035006 (2018).
- [42] W. Yantasee, Y. Lin, X. Li, G. E. Fryxell, T. S. Zemanian, and V. V. Viswanathan, Nanoengineered electrochemical sensor based on mesoporous silica thin-film functionalized with thiol-terminated monolayer, *Analyst* **128**, 899 (2003).
- [43] F. Guillemot, A. Brunet-Bruneau, E. Bourgeat-Lami, T. Gacoin, E. Barthel, and J.-P. Boilot, Latex-templated silica films:

- Tailoring porosity to get a stable low-refractive index, *Chem. Mater.* **22**, 2822 (2010).
- [44] F. Guillemot, Couches poreuses de silice structurées par des latex: Structure, propriétés mécaniques et applications optiques, Ph.D. thesis, Ecole Polytechnique, 2010.
- [45] L. Liskay, F. Guillemot, C. Corbel, J.-P. Boilot, T. Gacoin, E. Barthel, P. Pérez, M.-F. Barthe, P. Desgardin, P. Crivelli, U. Gendotti, and A. Rubbia, Positron annihilation in latex-templated macroporous silica films: Pore size and ortho-positronium escape, *New J. Phys.* **14**, 065009 (2012).
- [46] P. J. Schultz and K. G. Lynn, Interaction of positron beams with surfaces, thin films, and interfaces, *Rev. Mod. Phys.* **60**, 701 (1988).
- [47] O. E. Mogensen, Spur reaction model of positronium formation, *J. Chem. Phys.* **60**, 998 (1974).
- [48] M. Eldrup, A. Vehanen, P. J. Schultz, and K. G. Lynn, Positronium Formation and Diffusion in a Molecular Solid Studied with Variable-Energy Positrons, *Phys. Rev. Lett.* **51**, 2007 (1983).
- [49] S. Van Petegem, C. Dauwe, T. Van Hoecke, J. De Baerdemaeker, and D. Segers, Diffusion length of positrons and positronium investigated using a positron beam with longitudinal geometry, *Phys. Rev. B* **70**, 115410 (2004).
- [50] L. Liskay, C. Corbel, P. Perez, P. Desgardin, M. F. Barthe, T. Ohdaira, R. Suzuki, P. Crivelli, U. Gendotti, A. Rubbia, M. Etienne, and A. Walcarius, Positronium reemission yield from mesostructured silica films, *Appl. Phys. Lett.* **92**, 063114 (2008).
- [51] D. B. Cassidy, Experimental progress in positronium laser physics, *Eur. Phys. J. D* **72**, 53 (2018).
- [52] D. B. Cassidy, P. Crivelli, T. H. Hisakado, L. Liskay, V. E. Meline, P. Perez, H. W. K. Tom, and A. P. Mills, Jr., Positronium cooling in porous silica measured via Doppler spectroscopy, *Phys. Rev. A* **81**, 012715 (2010).
- [53] P. Crivelli, U. Gendotti, A. Rubbia, L. Liskay, P. Perez, and C. Corbel, Measurement of the ortho-positronium confinement energy in mesoporous thin films, *Phys. Rev. A* **81**, 052703 (2010).
- [54] S. M. Curry, Combined zeeman and motional stark effects in the first excited state of positronium, *Phys. Rev. A* **7**, 447 (1973).
- [55] K. P. Ziock, C. D. Dermer, R. H. Howell, F. Magnotta, and K. M. Jones, Optical saturation of the $1^3S - 2^3P$ transition in positronium, *J. Phys. B* **23**, 329 (1990).
- [56] A. M. Alonso, B. S. Cooper, A. Deller, S. D. Hogan, and D. B. Cassidy, Positronium decay from $n = 2$ states in electric and magnetic fields, *Phys. Rev. A* **93**, 012506 (2016).
- [57] A. Deller, B. S. Cooper, T. E. Wall, and D. B. Cassidy, Positronium emission from mesoporous silica studied by laser-enhanced time-of-flight spectroscopy, *New J. Phys.* **17**, 043059 (2015).
- [58] H. Saito, Y. Nagashima, T. Hyodo, and T. Chang, Detection of paramagnetic centers on amorphous-SiO₂ grain surfaces using positronium, *Phys. Rev. B* **52**, R689 (1995).
- [59] H. Saito and T. Hyodo, Quenching of positronium by surface paramagnetic centers in ultraviolet- and positron-irradiated fine oxide grains, *Phys. Rev. B* **60**, 11070 (1999).
- [60] Y. Nagashima, Y. Morinaka, T. Kurihara, Y. Nagai, T. Hyodo, T. Shidara, and K. Nakahara, Origins of positronium emitted from SiO₂, *Phys. Rev. B* **58**, 12676 (1998).
- [61] Y. Nagashima, M. Kakimoto, T. Hyodo, K. Fujiwara, A. Ichimura, T. Chang, J. Deng, T. Akahane, T. Chiba, K. Suzuki, B. T. A. McKee, and A. T. Stewart, Thermalization of free positronium atoms by collisions with silica-powder grains, aerogel grains, and gas molecules, *Phys. Rev. A* **52**, 258 (1995).
- [62] D. B. Cassidy, M. W. J. Bromley, L. C. Cota, T. H. Hisakado, H. W. K. Tom, and A. P. Mills, Jr., Cavity Induced Shift and Narrowing of the Positronium Lyman- α Transition, *Phys. Rev. Lett.* **106**, 023401 (2011).
- [63] G. F. Gribakin, J. A. Young, and C. M. Surko, Positron-molecule interactions: Resonant attachment, annihilation, and bound states, *Rev. Mod. Phys.* **82**, 2557 (2010).
- [64] M. W. Karl, H. Nakanishi, and D. M. Schrader, Chemical stability of positronic complexes with atoms and atomic ions, *Phys. Rev. A* **30**, 1624 (1984).
- [65] J. Mitroy, M. W. J. Bromley, and G. G. Ryzhikh, Positron and positronium binding to atoms, *J. Phys. B* **35**, R81 (2002).
- [66] X. Cheng, D. Babikov, and D. M. Schrader, Binding-energy predictions of positronium-atom systems, *Phys. Rev. A* **85**, 012503 (2012).
- [67] D. B. Cassidy and A. P. Mills, Jr., Enhanced Ps-Ps Interactions due to Quantum Confinement, *Phys. Rev. Lett.* **107**, 213401 (2011).
- [68] V. I. Goldanskii, The quenching of positronium and the inhibition of its formation (role of phase transitions, magnetic and chemical factors), in *Positron Annihilation*, edited by A. T. Stewart and L. O. Roellig (Academic, New York, 1967), pp. 183–255.
- [69] S. Y. Chuang and S. J. Tao, Quenching of positronium in nitrogen dioxide, *Phys. Rev. A* **9**, 989 (1974).
- [70] C. G. Fischer, M. H. Weber, C. L. Wang, S. P. McNeil, and K. G. Lynn, Positronium in low temperature mesoporous films, *Phys. Rev. B* **71**, 180102 (2005).
- [71] P. Sferlazzo, S. Berko, and K. F. Canter, Experimental support for physisorbed positronium at the surface of quartz, *Phys. Rev. B* **32**, 6067 (1985).
- [72] P. Sferlazzo, S. Berko, and K. F. Canter, Time-of-flight spectroscopy of positronium emission from quartz and magnesium oxide, *Phys. Rev. B* **35**, 5315 (1987).
- [73] A. Ishida, T. Namba, and S. Asai, Measurement of positronium thermalization in isobutane gas for precision measurement of ground-state hyperfine splitting, *J. Phys. B* **49**, 064008 (2016).
- [74] T. Chang, M. Xu, and X. Zeng, Effect of the energy loss process on the annihilation of ortho-positronium in silica aerogel, *Phys. Lett. A* **126**, 189 (1987).
- [75] M. Skalsey, J. J. Engbrecht, R. K. Bithell, R. S. Vallery, and D. W. Gidley, Thermalization of Positronium in Gases, *Phys. Rev. Lett.* **80**, 3727 (1998).
- [76] K. Shibuya, Y. Kawamura, and H. Saito, Time-resolved determination of ortho-positronium kinetic energy utilizing p -wave scattering during positronium-xenon collisions, *Phys. Rev. A* **88**, 042517 (2013).
- [77] C. He, T. Ohdaira, N. Oshima, M. Muramatsu, A. Kinomura, R. Suzuki, T. Oka, and Y. Kobayashi, Evidence for pore surface dependent positronium thermalization in mesoporous silica/hybrid silica films, *Phys. Rev. B* **75**, 195404 (2007).
- [78] C. He, T. Oka, Y. Kobayashi, N. Oshima, T. Ohdaira, A. Kinomura, and R. Suzuki, Positronium annihilation and pore surface chemistry in mesoporous silica films, *Appl. Phys. Lett.* **91**, 024102 (2007).
- [79] C. He, S. Wang, Y. Kobayashi, T. Ohdaira, and R. Suzuki, Role of pore morphology in positronium diffusion in mesoporous silica

- thin films and in positronium emission from the surfaces, [Phys. Rev. B **86**, 075415 \(2012\)](#).
- [80] C. He, B. Xiong, W. Mao, Y. Kobayashi, T. Oka, N. Oshima, and R. Suzuki, On determining the entrance size of cage-like pores in mesoporous silica films by positron annihilation lifetime spectroscopy, [Chem. Phys. Lett. **590**, 97 \(2013\)](#).
- [81] K. Shu, X. Fan, T. Yamazaki, T. Namba, S. Asai, K. Yoshioka, and M. Kuwata-Gonokami, Study on cooling of positronium for Bose Einstein condensation, [J. Phys. B **49**, 104001 \(2016\)](#).
- [82] P. M. Platzman and A. P. Mills, Jr., Possibilities for Bose condensation of positronium, [Phys. Rev. B **49**, 454 \(1994\)](#).